THE JOURNAL OF BIOLOGICAL CHEMISTRY VOL. 283, NO. 18, pp. 11924–11934, May 2, 2008

BAF60a Interacts with p53 to Recruit the SWI/SNF Complex*

Received for publication, July 2, 2007, and in revised form, February 26, 2008 Published, JBC Papers in Press, February 26, 2008, DOI 10.1074/jbc.M705401200

Jaehak Oh[‡1], **Dong H. Sohn**[‡1], **Myunggon Ko**[‡1], **Heekyoung Chung**[§], **Sung H. Jeon**[¶], **and Rho H. Seong**[‡2]

From the [‡]*Department of Biological Sciences, Institute of Molecular Biology and Genetics, and Research Center for Functional Cellulomics, Seoul National University, Seoul 151-742, Korea, the* [§]*Department of Pathology, College of Medicine, Hanyang University, Seoul 133-791, Korea, and the* [¶]*Department of Life Science and Institute of Bioscience and Biotechnology, Hallym University, Chuncheon 200-702, Korea*

To understand the tumor-suppressing mechanism of the SWI/SNF chromatin remodeling complex, we investigated its molecular relationship with p53. Using the pREP4-luc episomal reporter, we first demonstrated that p53 utilizes the chromatin remodeling activity of the SWI/SNF complex to initiate transcription from the chromatin-structured promoter. Among the components of the SWI/SNF complex, we identified BAF60a as a mediator of the interaction with p53 by the yeast two-hybrid assay. p53 directly interacted only with BAF60a, but not with other components of the SWI/SNF complex, such as BRG1, SRG3, SNF5, or BAF57. We found out that multiple residues at the amino acid 108–150 region of BAF60a were involved in the interaction with the tetramerization domain of p53. The N-terminal fragment of BAF60a containing the p53-interacting region as well as small interfering RNA for *baf60a* inhibited the SWI/SNF complex-mediated transcriptional activity of p53. The uncoupling of p53 with the SWI/SNF complex resulted in the repression of both p53-dependent apoptosis and cell cycle arrest by the regulation of target genes. These results suggest that the SWI/SNF chromatin remodeling complex is involved in the suppression of tumors by the interaction with p53.

The SWI/SNF complex is an ATP-dependent chromatin remodeling complex that alters the location or conformation of nucleosomes by using the energy of ATP hydrolysis (1). It is recruited to the promoter region of a target gene by the specific transcription factor and remodels the nucleosomes nearby to facilitate or repress transcription (2). The chromatin remodeling activity of the SWI/SNF complex is essential for developmental processes, hormone responses, and tumor suppression (3–5). The SWI/SNF complex is a multisubunit complex that consists of 9–12 subunits (6, 7). Among the components, BRG1 and BRM are the catalytic subunits with the ATPase domain, which alters the DNA-histone interaction. SRG3, the mouse homologue of human BAF155, is a scaffold protein that controls the stability of the complex by interaction with other components (8). SNF5 and BAF57 have a mediating function of recruiting transcription factors to the SWI/SNF complex (9–11). BAF60 has three isoforms, BAF60a, BAF60b, and BAF60c. They show different expression patterns among tissues and interact with different combinations of nuclear receptors as a mediator (6, 12, 13). In the case of BAF60a, not only various nuclear receptors but also nonreceptor nuclear proteins, such as AP-1 and FEZ1, have been shown to associate with BAF60a to utilize the SWI/SNF complex (12, 14–16). Since BAF60a has been revealed as a mediator with the versatility to interact with various forms of transcription factors and the N terminus has been mapped to be the interface for the interaction, the mechanism of the versatility of BAF60a is becoming an interesting question (12–14, 16, 17).

The chromatin-remodeling mechanism of the SWI/SNF complex has been best described with the transcriptional activity of nuclear receptors. Since chromatin structures play a repressive role in the control of transcriptional regulation (18), nuclear receptors utilize the SWI/SNF complex to unravel and activate the chromatin-structured promoters upon hormone stimulation (19). The requirement of the remodeling activity of the SWI/SNF complex on the transactivity of glucocorticoid receptor (GR)[3] has been demonstrated with the mouse mammary tumor virus (MMTV) long terminal repeat (LTR) promoter (19). The hormone response elements (HRE) in LTR, which are responsible for the transcriptional response to hormones, such as glucocorticoid and testosterone, are concealed in the nucleosomal array when MMTV LTR is stably integrated. GR initiates transcription from the chromatin-structured MMTV LTR by using the SWI/SNF complex on the hormone stimulation. Thus, when the wild-type BRG1 is substituted by the chromatin remodeling-deficient BRG1 mutants or the interaction between GR and the SWI/SNF complex is disrupted, the chromatin-structured MMTV LTR is not remodeled and therefore not activated by hormone stimulation (12, 20). Besides this remodeling function of the SWI/SNF complex, general cofactor activity of the complex is also suggested. For example, substitution of BRG1 by the chromatin remodeling-deficient BRG1 mutants, which are not able to induce tran-

* This work was supported in part by a grant from the Korea Science and Engineering Foundation through the Research Center for Functional Cellulomics (to R. H. S.). The costs of publication of this article were defrayed in part by the payment of page charges. This article must therefore be hereby marked "*advertisement*" in accordance with 18 U.S.C. Section 1734 solely to indicate this fact.

[1] These authors were supported by the BK21 Program from Ministry of Education and Human Resources Development.

[2] To whom correspondence should be addressed: Dept. of Biological Sciences, Institute of Molecular Biology and Genetics (Bldg. 105) and Research Center for Functional Cellulomics, Seoul National University, San 56-1, Shinlim-dong, Kwanak-gu, Seoul, 151-742, Republic of Korea. Tel.: 82-2-880-7567; Fax: 82-2-878-9380; E-mail: rhseong@snu.ac.kr.

[3] The abbreviations used are: GR, glucocorticoid receptor; MMTV, mouse mammary tumor virus; LTR, long terminal repeat; HRE, hormone response element(s); AR, androgen receptor; PI, propidium iodide; RT, reverse transcription; DBD, DNA binding domain; aa, amino acid(s); GFP, green fluorescent protein.

scription from the stably integrated MMTV LTR, can activate the transiently transfected MMTV-LTR promoter as efficiently as wild-type BRG1 (20). Furthermore, overexpression of SRG3 alone is also capable of enhancing the transcriptional activity of androgen receptor (AR) even in a BRG1-null cell line (21). Thus, a refined system is needed to study the mechanism of the SWI/SNF complex-mediated activation precisely.

p53 is a tumor suppressor protein that plays a critical role in mediating cellular response to stress (22). It is well known that p53 exerts the tumor suppressor effect mainly by its transcriptional activity. Recruitment of many cofactors, such as p300/CBP, HAT, HDAC, CARM1, and PRMT1, that modify histones is crucial for p53 to regulate the expression of target genes (23–26). Recently, Lee *et al.* have shown that the components of the SWI/SNF complex can interact with p53 (27). They also reported enhancement of the p53 activity by overexpression of BRG1 and SNF5 of the SWI/SNF complex using the transiently transfected plasmid reporter. However, it is unclear whether the chromatin remodeling activity exerted by the SWI/SNF complex is actually required, since the transiently transfected plasmid reporter rarely forms a chromatin structure. It is also possible that the cofactor activity of BRG1 or SNF5 to recruit the general transcriptional machinery may enhance the transcriptional activity of p53 (20, 21). Therefore, the role of the SWI/SNF complex in the p53-mediated transcription remains to be carefully delineated.

Here, we characterized the interaction and cooperation between the SWI/SNF chromatin remodeling complex and p53 to understand the tumor-suppressing activity of the SWI/SNF complex. By using an episomal pREP4-luc reporter, we found that p53 utilizes the chromatin remodeling activity of the SWI/SNF complex. Although the core components of the SWI/SNF complex were co-immunoprecipitated with p53, only BAF60a was shown to interact directly with p53, whereas the other components did not in the yeast two-hybrid assays, suggesting BAF60a as a linker between the SWI/SNF complex and p53. After mapping the p53-interacting region on BAF60a in detail, we designed a dominant negative form of it (BAF60a160), which specifically disrupted the SWI/SNF complex-mediated transcriptional activity of p53. The dominant negative form of BAF60a as well as siRNA for *baf60a* attenuated the p53-dependent apoptosis and cell cycle arrest by inhibiting *bax* and *p21* expression. Collectively, our results demonstrate the cooperative role of the SWI/SNF complex for the p53-mediated anti-tumor functions.

EXPERIMENTAL PROCEDURES

Plasmids and Site-directed Mutagenesis—For cloning of the yeast two-hybrid vector, *flag-brg1*, *myc-srg3*, *flag-baf60a*, *ha-snf5, and ha-baf57* were PCR-amplified with primers containing N-terminal tag sequences and inserted into pGBKT7 vector in fusion with the GAL4-DNA binding domain. *flag-p53* and *myc-srg3* were cloned in frame to pACT2 vector, which has the GAL4 activation domain. Several oligonucleotides were designed for PCR amplification of deletion mutants of *baf60a* and *p53* based on NCBI sequences. The PCR-amplified fragments were inserted in frame into pGBKT7 and pACT2 vector, respectively. For mammalian expression plasmids, *flag-p53*, *ha-baf60a*, and *ha-baf60a* deletion mutants, including *ha-baf60a160* and *ha-baf60aΔ108–150*, were cloned into pcDNA3 vector, and *flag-brg1* and *ha-gr* were inserted into pCAGGS vector. pcDNA3-AR was a generous gift from Dr. K. Lee (Hormone Research Center, Chonnam National University, Gwangju, Korea). *baf60a160* was inserted to MigRI retroviral vector for viral transduction. For the interference of *baf60a* mRNA, pSilencer1.0-U6 siRNA expression vector was used. 5′-AATCGAAATCACAATGCAA-3′ is the target sense sequence designed for si-*baf60a*. pTK-*Hyg* vector was used for selection of cells that are resistant to hygromycin B. pREP4-p53RE-luc and pREP4-MMTV-luc reporter were constructed by inserting p53-responsive elements and the LTR of MMTV, respectively into pREP4-luc episomal vector, which forms chromatin structure when transiently transfected in cells (from Dr. Keji Zhao, NHLBI, National Institutes of Health, Bethesda, MD). *baf60a* internal deletion mutants were generated using the QuikChange site-directed mutagenesis kit (Stratagene, La Jolla, CA) according to the manufacturer's instructions. All of the genes used in this study were from mouse cDNA. The sequence correctness, orientation, and frame correctness of each plasmid were confirmed by automated sequencing.

Cell Culture and Establishment of Stable Cell Lines—SaOS-2, SW-13, COS-1, 293T, and Phoenix cell lines were cultured in Dulbecco's modified Eagle's medium containing 10% fetal bovine serum. NIH3T3 was cultured in Dulbecco's modified Eagle's medium supplemented with 10% BCS, and the LNCaP cell line was cultured in Iscove's modified Eagle's medium supplemented with 10% fetal bovine serum. For the establishment of NIH3T3-U6 and NIH3T3-U6-si-BAF60a cells that have stably integrated pSilencer-U6 and pSilencer-U6-si-BAF60a vectors, respectively, NIH3T3 cells were split into two 60-mm dishes, 18–24 h before transfection. Then 1 μg of pTK-*Hyg* vector was co-transfected with 10 μg of pSilencer1.0-U6 or pSilencer1.0-U6-si-BAF60a, respectively. 48 h after the transfection, the cells were treated with hygromycin B (200 μg/ml). The medium was replaced with fresh medium containing 200 μg/ml hygromycin B every 3–4 days, and this selection process lasted for 3 weeks to generate pooled stable cells.

Transfection, Retroviral Transduction, and Luciferase Assay—Transfection experiments were performed by the $CaPO_4$ method except for the establishment of stable cells and the transfection of the LNCaP cell line. Those cell lines were transfected with Lipofectamine2000 (Invitrogen). Retroviral transduction was carried out as described previously (44). Appropriate mock DNA, an empty vector, was supplemented to adjust the total DNA amount in all groups. For luciferase assay, the luciferase activity was assayed according to the manufacturer's protocol (Promega, Madison, WI). CMV-LacZ plasmid was co-transfected, and β-galactosidase activity was measured to normalize the transfection efficiency.

Antibodies, Immunoprecipitation, and Immunoblotting—For immunoprecipitation experiments, whole cell extracts or nuclear extracts were prepared as previously described (28). 500 μg of extracts were diluted into 500 μl with Buffer X and precleared once with 40 μl of 50% protein A- or G-Sepharose (Amersham Biosciences) at 4 °C for 1 h (29). The designated antibody was incubated with the supernatant for 3 h at 4 °C and

then with protein A- or G-Sepharose for 1 h. The immunoprecipitated complexes were washed three times with 500 μl of HEGNDT buffer (10 mM HEPES, pH 8.0, 1 mM EDTA, 10% glycerol, 50 mM NaCl, 2 mM dithiothreitol, 0.1% Triton X-100) and once with HEGND buffer (HEGNDT buffer without Triton X-100). The washed pellets were eluted with SDS-PAGE loading buffer and boiled for 4 min. For immunoblot analysis, proteins were resolved by SDS-PAGE and transferred to Immobilon-P membrane (Millipore). Anti-FLAG (M2; Sigma), anti-HA (HA-7; Sigma), anti-BAF60a (Transduction Laboratories, Lexington, KY), anti-β-actin (AC-15; Sigma), anti-p53 (FL393 and DO-1; Santa Cruz Biotechnology, Inc., Santa Cruz, CA), anti-p21 (BD Biosciences), and annexin V-PE (BD Biosciences) antibodies were purchased commercially, and antisera against SRG3 and BRG1 were raised from rabbits in our laboratory.

Yeast Two-hybrid Assay and Yeast Extract Preparation—After overnight growing on YPDA, a rich plate, at 30 °C, the same amount of AH109 yeasts was co-transformed with 1 μg of each set of plasmids in pGBKT7 and pACT2. Since this strain cannot synthesize tryptophan, leucine, adenine, and histidine by itself, all of these four nutrients were supplemented exogenously to yield colonies. Tryptophan and leucine were supplemented by the presence of the pGBKT7 and pACT2 vectors, respectively, and adenine and histidine were supplemented through the separate GAL1 and GAL2 reporter when prey and bait interacted. Co-transformed yeast was grown on a selection plate without tryptophan, leucine, adenine, and histidine and incubated at 30 °C for a week. The number of colonies that appeared was counted to measure interaction strength. For preparation of yeast extract, we used the urea/SDS method as per the manufacturer's instructions (Clontech). The extracts were analyzed by Western blotting.

Annexin V and Propidium Iodide (PI) Staining and Flow Cytometry—For annexin V staining, cells were washed twice with phosphate-buffered saline and stained with annexin V-PE antibody according to the manufacturer's instruction. For PI staining, cells were washed twice with phosphate-buffered saline, fixed with 70% ethanol for 30 min at 4 °C, and then harvested to stain with PI solution for 30 min at room temperature. Flow cytometry was carried out using a FACSCaliber (BD Biosciences), and data were analyzed by CellQuest software (BD Biosciences).

RNA Isolation and Reverse Transcription (RT)-PCR—Total RNA was prepared with TRIzol reagent (Invitrogen), and 2 μg of total RNA was reverse-transcribed with oligo(dT) primer and Superscript III (Invitrogen) as instructed by the manufacturer. β-Actin was used as an internal control for RT-PCR analysis. Specific primers used for PCR were as follows: mouse *p21* (forward, 5′-CGGTGGAACTTTGACTTCGT-3′; reverse, 5′-CACAGAGTGAGGGCTAAGGC-3′), mouse *bax* (forward, 5′-TGCAGAGGATGATTGCTGAC-3′; reverse, 5′-GAGGACTCCAGCCACAAAGA-3′), human *p21* (forward, 5′-AAGACCATGTGGACCTGTCA-3′; reverse, 5′-GGCTTCCTCTTGGAGAAGAT-3′), human *bax* (forward, 5′-CCAGCTGCCTTGGACTGT-3′; reverse 5′-ACCCCCTCAAGACCACTCTT-3′), human β-actin (forward, 5′-GACAGCAGTCGGTTGGACC-3′; reverse, 5′-CAGGTAAGCCCTGGCTGC-3′), and mouse *gapdh* (forward, 5′-CAGACACCCAACTTTCGCAT-3′; reverse, 5′-TGTTCCGGGTGGTTCTGCAG-3′).

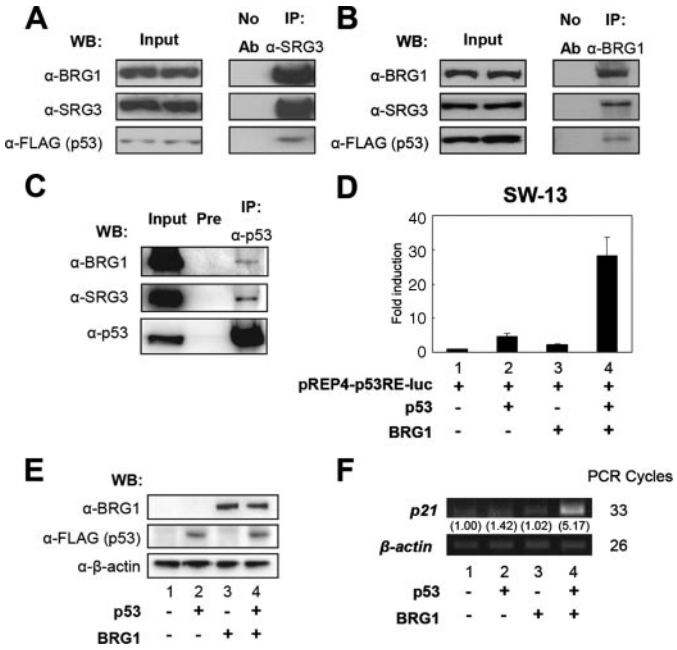

FIGURE 1. **p53 utilizes the chromatin remodeling activity of the SWI/SNF complex.** *A*, SaOS-2 cells were transfected with expression vector for FLAG-p53. The nuclear extracts (500 μg) were immunoprecipitated (*IP*) without (*No Ab*) or with (*α-SRG3*) anti-SRG3 antiserum and subjected to immunoblot analysis (*WB*) with antiserum for BRG1 (*top*) and SRG3 (*middle*) and anti-FLAG antibody (*bottom*). *B*, immunoprecipitation and immunoblot were performed as in *A*, but the immunoprecipitation assay was carried out with anti-BRG1 antiserum. *C*, 293T cells were treated with 1 μg/ml doxorubicin for 24 h to activate endogenous p53. Subsequently, nuclear extract (500 μg) was prepared and subjected to immunoprecipitation with anti-p53 antibody (*DO-1*). The Sepharose used in preclearing (*Pre*) was resolved in parallel with 50 μg of nuclear extracts (*Input*) and immunoprecipitants (*IP*) by SDS-PAGE. Anti-BRG1 antiserum (*top*), anti-SRG3 antiserum (*middle*), and anti-p53 antibody (*bottom*) were used for immunoblotting as indicated. *D*, the pREP4-p53RE-luc episomal reporter was co-transfected with expression vectors for FLAG-BRG1 (9 μg) and FLAG-p53 (3 μg) in SW-13 cells as indicated. The luciferase activity was measured, and the relative activities of three independent experiments are presented with S.D. values (*lane 1* set as 1-fold). *E* and *F*, FLAG-BRG1 (9 μg) and FLAG-p53 (3 μg) were transfected as indicated *below* the *panels*. Cells were harvested, and each sample was split into two separate tubes. Whole cell extracts of one set were Western blotted with anti-BRG1 antiserum (*top*), anti-FLAG antibody (*middle*), and anti-β-actin antibody (*bottom*) (*E*). Total RNAs of the other set were extracted and were subjected to RT-PCR with primers for *p21* after standardization with β-actin primer (*F*). The *numbers* in *parenthesis* mean relative value of the mRNA level of *p21*. PCR cycles are indicated at the *right*.

RESULTS

p53 Utilizes the Chromatin Remodeling Activity of the SWI/SNF Complex—We first tested whether the transcriptional activity of p53 is dependent on the chromatin remodeling activity of the SWI/SNF complex. We examined whether p53 and the SWI/SNF complex interact in the nucleus. SaOS-2 cells, which lack p53 but express the SWI/SNF complex, were transfected with FLAG-p53, and nuclear extracts were subjected to an immunoprecipitation assay with antiserum against SRG3 and BRG1. FLAG-p53 specifically co-immunoprecipitated with both SRG3 and BRG1, the core components of the SWI/SNF complex (Fig. 1, *A* and *B*). Next, we investigated interaction between the endogenous proteins. When an immunoprecipitation assay was performed with anti-p53 antibody, both BRG1

and SRG3 were co-purified with p53, which was endogenously induced by the treatment of doxorubicin, the DNA-damaging agent (Fig. 1*C*). These results suggest the nuclear association between the SWI/SNF complex and p53.

Previously, the transcriptional activity of p53 was reported to be enhanced by overexpression of the components of the SWI/SNF complex (27). However, this enhancement could be due to either the general cofactor activity of the components or the chromatin remodeling activity of the complex. To distinguish between these two possibilities, we employed a pREP4-luc reporter. This episomal reporter has previously been shown to form a nucleosomal structure and stringently require the SWI/SNF chromatin remodeling activity to be remodeled and activated (32–34). We constructed the pREP4-p53RE-luc reporter, which contains p53-responsive elements in the promoter. The reporter assay was performed in SW-13 cells, because this cell line has a nonfunctional SWI/SNF complex due to the lack of the BRG1 subunit but is capable to restore functional SWI/SNF complex upon BRG1 expression (35). Transfection of neither p53 (4-fold) nor BRG1 expression vector (2-fold) alone induced a significant amount of luciferase activity from the pREP4-p53RE-luc reporter (Fig. 1*D*, *lanes 2* and *3 versus lane 1*). However, when BRG1 was co-expressed with p53, the reporter gene activity was increased 28-fold without increasing the expression level of p53 (Fig. 1, *D* (*lane 4*) and *E*). This was not due to a p53-independent activation of the reporter by the SWI/SNF complex, because the expression of BRG1 alone did not induce luciferase activity (Fig. 1*D*, *lane 3*). Subsequently, we examined if p53-mediated transcription of the target gene actually utilizes the SWI/SNF chromatin remodeling complex. Similar to the result obtained from the pREP4-luc reporter assay, expression of *p21*, the target gene of p53, was enhanced in the presence of both BRG1 and p53 but not with either p53 or BRG1 alone in the SW-13 cell line (Fig. 1*F*). These results indicate that the chromatin remodeling activity of the SWI/SNF complex is required for p53 to initiate transcription from the chromatin-structured promoter.

BAF60a Mediates the Interaction between the SWI/SNF Complex and p53—To identify the component(s) of the SWI/SNF complex interacting directly with p53, we performed the yeast two-hybrid assays between subunits of the SWI/SNF complex and p53. We cloned *p53* in the GAL4 activation domain (GAL4-AD)-containing vector (pACT2) and *brg1*, *srg3*, *baf60a*, *snf5*, and *baf57* in the GAL4-DNA binding domain (GAL4-DBD)-containing vector (pGBKT7) in frame. Each cloned plasmid was co-transformed with a matching mock vector, resulting in no false-positive colonies. Then each GAL4-DBD-SWI/SNF component was co-transformed with GAL4-AD-p53. On average, about 1000 colonies appeared only in *baf60a* construct, but no colonies were observed in any other subunit constructs. Surprisingly, BRG1 and SNF5, which were previously reported to interact with p53 by the glutathione *S*-transferase pull-down assay (27), did not interact directly with p53 in our yeast two-hybrid assays. In order to exclude the possibility that the transformed *brg1* and *snf5* constructs were neither expressed nor functional, we carried out the Western blot analysis with *brg1*- and *snf5*-transformed yeast extracts. Both GAL4-DBD-BRG1 and GAL4-DBD-SNF5 plasmids were found to be expressed well in the transformed yeasts (data not shown). Furthermore, when we co-transformed each of them with the GAL4-AD-SRG3 which is known to interact directly with both of them (8), colonies were observed as reported, suggesting that they are functional in yeast for the assay (data not shown). These results suggest that the interaction between the SWI/SNF complex and p53 is indirect, except for BAF60a, although other components of the SWI/SNF complex, such as BRG1, SNF5, and SRG3, have also been co-immunoprecipitated with p53 (27) (Fig. 1, *A–C*). To confirm the interaction between p53 and BAF60a also in mammalian systems, we co-transfected mammalian expression plasmids of HA-BAF60a and FLAG-p53 in the COS-1 cell line and performed reciprocal immunoprecipitation assays with both anti-FLAG and anti-HA antibodies. As shown in Fig. 2*A*, the interaction between exogenous p53 and BAF60a was confirmed by reciprocal co-immunoprecipitation in mammalian cells. Next, we examined the nuclear association between the endogenous BAF60a and p53. After the treatment of doxorubicin to induce endogenous p53 in the 293T cell line, the nuclear extracts were immunoprecipitated with anti-BAF60a antibody. As shown in Fig. 2*B*, endogenous p53 as well as BRG1 and SRG3 co-immunoprecipitated with endogenous BAF60a. These results suggest that the interaction between BAF60a and p53 is formed not only in yeast but also in the nucleus of mammalian cells.

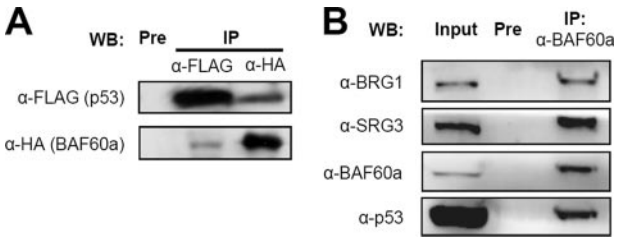

FIGURE 2. **BAF60a interacts with p53.** *A*, COS-1 cells were transfected with FLAG-p53 and HA-BAF60a expression vectors. At 36 h post-transfection, whole cell extracts (500 μg) were immunoprecipitated with antibody for FLAG or HA. The immunoprecipitants (*IP*) were immunoblotted (*WB*) with anti-FLAG (*top*) and anti-HA (*bottom*) antibodies in parallel with eluates from the Sepharose used in preclearing (*Pre*). *B*, 24 h after the treatment of 1 μg/ml doxorubicin in the 293T cell line, nuclear extracts (500 μg) were subjected to an immunoprecipitation assay with antibody for endogenous BAF60a. The Sepharose used in preclearing was resolved in parallel with 50 μg of nuclear extracts (*Input*) and immunoprecipitants by SDS-PAGE. Anti-BRG1 antiserum (*top panel*), anti-SRG3 antiserum (*upper middle panel*), anti-BAF60a antibody (*lower middle panel*), and anti-p53 antibody (*bottom panel*) were used for immunoblotting of BRG1, SRG3, BAF60a, and p53, respectively.

Multiple Residues in Amino Acids 108–150 of BAF60a Are Implicated in the Interaction with p53—We mapped the p53-interacting region on BAF60a using the yeast two-hybrid assay. There is the SWIB/MDM2 domain on BAF60a, which is known to fold like the p53-interacting region of MDM2, the master regulator of p53 (36). Thus, we considered this domain as a putative candidate for the p53-interacting region and constructed C-terminal serial deletion mutants of *baf60a* into the GAL4-DBD vector to perform the yeast two-hybrid assays with GAL4-AD-p53. Until deletion to amino acid 126 from the C terminus, interaction strengths of BAF60a 1–251, BAF60a 1–160, and BAF60a 1–126 with p53 were similar to that of wild-type BAF60a (Fig. 3*A*). BAF60a 1–113 interacted, but only weakly, with p53, whereas none of the BAF60a 1–107 and fur-

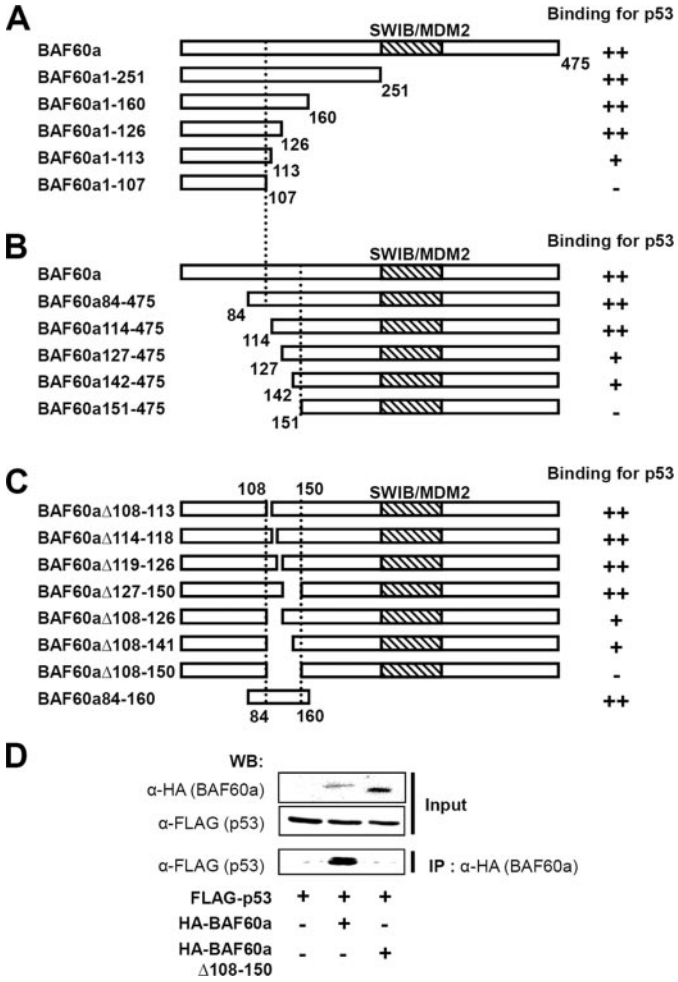

FIGURE 3. **Mapping of the p53-interacting region on BAF60a.** *A*, the interactions between various deletion mutants of BAF60a and p53 were analyzed by the yeast two-hybrid assay. The schematic drawing of *baf60a* deletion mutants fused to GAD4-DBD is depicted. The *diagonally striped box* represents the SWIB/MDM2 domain, and the *numbers below* the *bars* represent amino acid residues of each end. The *dotted line* indicates the border of the p53-interacting regions identified by each set of experiments. Serial C-terminal deletion mutants of *baf60a* in pGBKT7 vector were co-transformed with pACT2-p53 for the yeast two-hybrid assays. Binding strengths of the deletion mutants of BAF60a for p53 were measured by the colony number relative to wild-type BAF60a and are represented by *minus* or *plus signs* on the *right* under *Binding for p53*; −, no colony; +, <50% of colonies with wild-type BAF60a; ++, >80% of colonies with wild-type BAF60a. *B*, serial N-terminal deletion mutants of *baf60a* in pGBKT7 vector were co-transformed with pACT2-p53 for the yeast two-hybrid assay, and the binding strength was measured and presented as above. *C*, internal deletion mutants of *baf60a* and *baf60a* aa 84–160 (*BAF60a84–160*) in pGBKT7 vector were co-transformed with pACT2-p53 for the yeast two-hybrid assay. The interactions were measured and presented as above. *D*, empty, HA-BAF60a, or HA-BAF60aΔ108–150 expression vector was co-transfected with expression vector for FLAG-p53 into COS-1 cells. At 36 h post-transfection, whole cell extracts (500 μg) were prepared and subjected to an immunoprecipitation assay with anti-HA antibody. Immunoprecipitants (*IP*) and 50 μg of input (*Input*) were immunoblotted (*WB*) with anti-HA (*top*) and anti-FLAG (*middle* and *bottom*) antibodies.

ther deletion mutants interacted with p53 (Fig. 3*A*) (data not shown). Thus, the amino acid (aa) 108–126 region of BAF60a appeared to be implicated in the interaction with p53. We next cloned N-terminal serial deletion mutants of *baf60a* in the GAL4-DBD vector and performed the yeast two-hybrid assays again with GAL4-AD-p53 in order to exclude the possibility that the C-terminal region of BAF60a, including the SWIB/MDM2 domain, is involved in the interaction with p53. BAF60a 114–475 without aa 108–113 even interacted with p53 as efficiently as wild-type BAF60a. Strikingly, despite the lack of aa 108–126, BAF60a 127–475 and BAF60a 142–475 were able to interact with p53, although weakly, suggesting the presence of an additional interacting region(s) (Fig. 3*B*). However, BAF60a 151–475 and further deletion mutants did not interact with p53 (Fig. 3*B*) (data not shown). Taken together, the aa 108–150 region of BAF60a, but not the SWIB/MDM2 domain, seems to be involved in the interaction with p53. To rule out the misfolding or insolubilization problem of the terminal deletion mutants, we constructed several internal deletion mutants of *baf60a* within aa 108–150 into the GAL4-DBD vector and performed the yeast two-hybrid assays with GAL4-AD-p53. As shown in Fig. 3*C*, BAF60aΔ108–150, in which the p53-interacting region was completely deleted, did not interact with p53 at all, whereas none of the partial deletion mutants in this region completely abrogated the interaction with p53. These results correlate well with the results of the N- and C-terminal deletion studies. In addition, BAF60a 84–160, which contains the entire aa 108–150 region, was able to interact with p53 as strongly as wild-type despite being the shortest deletion mutant (Fig. 3*C*). aa 108–150 region-dependent interaction of BAF60a with p53 was also observed in a mammalian system. The mammalian expression vector for FLAG-p53 was co-transfected with mock, HA-BAF60a, or HA-BAF60aΔ108–150 expression vector into the COS-1 cell line, and immunoprecipitation assays were carried out with anti-HA antibody. p53 did specifically immunoprecipitate with BAF60a as shown in Fig. 2*A*, whereas p53 did not co-precipitate with BAF60aΔ108–150 (Fig. 3*D*). Taken together, multiple residues within aa 108–150 of BAF60a are implicated in the interaction with p53.

Tetramerization Domain of p53 Interacts with BAF60a—We next investigated the BAF60a-interacting region of p53. The functional domains of p53 have already been defined. The transactivation domain is at the N terminus (aa 1–43), and the DNA-binding domain is in the middle of the protein (aa 110–286). The tetramerization domain and the regulatory domain are located at the C terminus (aa 326–355 and 364–391, respectively). Thus, we cloned deletion mutants of p53, p53 1–299, p53 51–391, p53 51–299, p53 300–391, and p53 364–391, into the GAL4-AD vector based on the domain structure of p53. In the yeast two-hybrid assays with GAL4-DBD-BAF60a, p53 1–299, p53 51–299, and p53 364–391 did not interact with BAF60a, whereas p53 51–391 and p53 300–391 interacted as efficiently as wild-type p53 (Fig. 4). Therefore, aa 300–363, which includes the tetramerization domain of p53, is required for the interaction with BAF60a.

Down-regulation of BAF60a Reduces the SWI/SNF Complex-mediated Transcriptional Activity of p53—To examine the function of BAF60a in mediating the SWI/SNF complex-mediated transcriptional activity of p53, we attempted to down-regulate endogenous BAF60a in NIH3T3 cells that express the functional SWI/SNF complex, including BAF60a. For significant down-regulation of BAF60a in protein level, we established NIH3T3-U6-si-BAF60a cells that stably express si-*baf60a* and NIH3T3-U6 cells that contain mock vector. NIH3T3-U6-si-BAF60a cells showed decreased BAF60a in pro-

FIGURE 4. **Mapping of the BAF60a-interacting region on p53.** The interactions between BAF60a and deletion mutants of p53 were analyzed. The schematic drawing of p53 deletion mutants fused to GAD4-AD is depicted. *p53* deletion mutants in pACT2 vector were subjected to the yeast two-hybrid assay with pGBKT7-BAF60a. Transactivation domain (*TA*), DNA-binding domain (*DNA-BD*), tetramerization domain (*TD*), and regulatory domain (*RD*) of p53 are indicated, and the *numbers below* the *bars* represent amino acid residues of each end. Binding strength was measured by the relative colony number and is represented on the *right* under *Binding for BAF60a*; −, no colony; ++, >80% of colonies with wild-type p53.

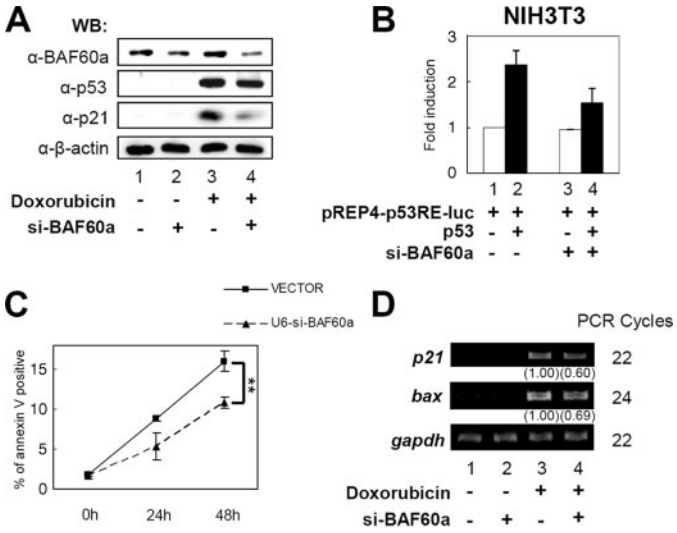

FIGURE 5. **Knockdown of BAF60a represses the SWI/SNF complex-mediated activation of p53.** *A*, NIH3T3-U6 (−) and NIH3T3-U6-si-BAF60a (+) cells were treated with vehicle (−) or 1 μg/ml doxorubicin (+) for 24 h. Cell extracts were performed for immunoblotting with anti-BAF60a, anti-p53, anti-p21, and anti-β-actin antibody as indicated. *B*, NIH3T3-U6 and NIH3T3-U6-si-BAF60a cells were co-transfected with pREP4-p53RE-luc (3 μg) and *p53* (1 μg) as indicated below. After 36 h post-transfection, luciferase activity was measured, and the relative activities of three independent experiments are presented with S.D. values (*lane 1* set as 1-fold). *C*, NIH3T3-U6 and NIH3T3-U6-si-BAF60a cells were treated with 1 μg/ml doxorubicin, harvested at the indicated time points, and stained with annexin V-PE antibody to analyze with flow cytometry. **, significance at 48 h time point; $p < 0.01$ for *t* test. *D*, after 48 h of treatment with vehicle (−) or 1 μg/ml doxorubicin (+) in NIH3T3-U6 (−) and NIH3T3-U6-si-BAF60a (+) cells, total RNAs were extracted and subjected to RT-PCR with primers specific for the genes shown on the *left* of each *panel* after standardization with *gapdh* primer. This is representative of three similar results. Relative values of the mRNA level are represented in *parenthesis*, and PCR cycles are indicated at the *right*.

tein level compared with NIH3T3-U6 cells (Fig. 5*A*, *top*, *lane 2 versus lane 1*). With these cells, we analyzed the effect of the reduced BAF60a on the SWI/SNF complex-mediated transcriptional activity of p53. The pREP4-p53RE-luc reporter was co-transfected with or without p53 in NIH3T3-U6 and NIH3T3-U6-si-BAF60a cell lines. Although the basal reporter activity was equal in both cells (Fig. 5*B*, *lane 1 versus lane 3*), the transcriptional activity of ectopic p53 was significantly repressed in NIH3T3-U6-si-BAF60a cells (Fig. 5*B*, *lane 2 versus lane 4*). To examine the knockdown effect of BAF60a on p53 target gene expression, we treated cells with doxorubicin to activate p53 and measured changes in the induction of *p21*. In the immunoblot analysis, p21 protein levels were reduced in NIH3T3-U6-si-BAF60a cells, whereas p53 protein induction was not different (Fig. 5*A*). Because prolonged exposure to doxorubicin induces apoptosis in the NIH3T3 cell line, we investigated if endogenous BAF60a is also required for p53-mediated apoptosis. We measured the percentage of annexin V-positive population by flow cytometry in both cells. Doxorubicin-induced apoptosis was repressed in NIH3T3-U6-si-BAF60a cells relative to NIH3T3-U6 cells at the 24 and 48 h time points (Fig. 5*C*). Because p53-mediated apoptosis was affected by the knockdown of BAF60a, we next examined changes in the expression of proapoptotic p53 target gene, *bax* (45). When assessed by RT-PCR, enhanced expression of both *p21* and *bax* (Fig. 5*D*, *lane 3 versus lane 1*) was clearly suppressed by knockdown of endogenous BAF60a (Fig. 5*D*, *lane 4 versus lane 3*). Taken together, these results suggest that knockdown of BAF60a may repress the transcriptional activity of p53 and thereby inhibit the p53-mediated tumor suppression function.

BAF60a160 Disrupts the SWI/SNF Complex-mediated Transcriptional Activity of p53—To further evaluate the importance of the p53-SWI/SNF complex interaction in the activation of p53-mediated transcription, we attempted to generate a dominant negative mutant of BAF60a. Based on the C-terminal deletion mutant study of Fig. 3*A*, BAF60a 1–160 (BAF60a160) was tested for its dominant negative activity, because it contains the p53-interacting region and has the potential to compete with the BAF60a in the SWI/SNF complex for binding to p53 (Fig. 3*A*, *BAF60a* and *BAF60a1–160*). This form of BAF60a mutant is known to disrupt the interaction between GR and the SWI/SNF complex (12). First, we examined whether BAF60a160 inhibits the p53-mediated chromatin remodeling activity of the SWI/SNF complex in the SW-13 cell line. In agreement with the results of Fig. 1*D*, the transcriptional activity of p53 on the pREP4-p53RE-luc reporter was enhanced about 10-fold by the co-expression of BRG1 in SW-13 cells (Fig. 6*A*, *lane 2 versus lane 1*). However, the SWI/SNF complex-mediated transcriptional activity of p53 was repressed by about half when BAF60a160 was co-expressed with BRG1 and p53 (Fig. 6*A*, *lane 3 versus lane 2*). Therefore, BAF60a160 acted in a dominant negative fashion and disrupted the SWI/SNF complex-mediated transcriptional activity of p53 in the SW-13 cell line. Next, we examined whether BAF60a160 suppresses the transcriptional activity of p53 in a dose-dependent manner. If BAF60a160 inhibits by competition with the SWI/SNF complex for p53, the transcriptional activity of p53 will be repressed further as the expression of BAF60a160 increases. In NIH3T3 cells, which have the functional SWI/SNF complex, co-expression of a fixed amount of p53 and increasing amount of BAF60a160 resulted in progressive down-regulation of the transcriptional activity of p53 (Fig. 6*B*, *lanes 3–5*). This was not due to the reduction of p53 expression, because the p53 expression was not repressed by co-expression of BAF60a160 (Fig. 6*C*). Similar results were also obtained in the SaOS-2 cell line (Fig. 6*D*). Therefore, these results indicate that BAF60a160 is a

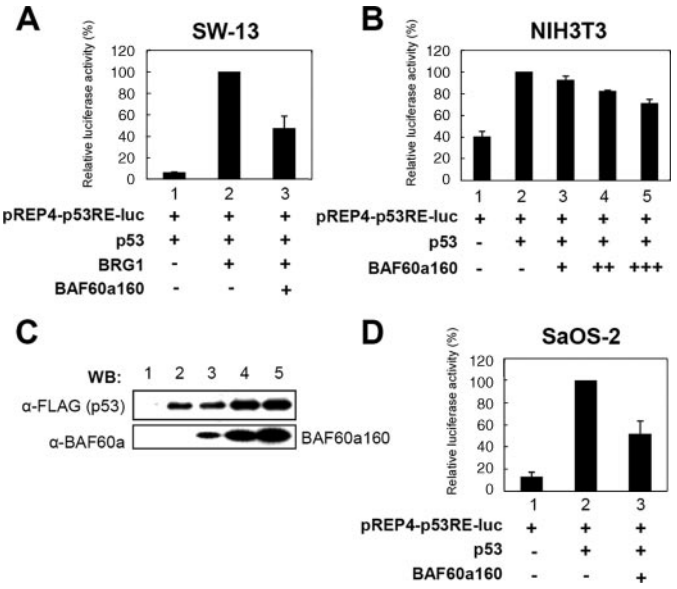

FIGURE 6. **BAF60a160 represses the transcriptional activity of p53.** *A*, the pREP4-p53RE-luc episomal reporter was transfected with expression vector for p53 (1 μg) in combination with BRG1 (3 μg) and BAF60a160 (10 μg) in SW-13 cells. Relative luciferase activities due to p53 are presented as a percentage of the SWI/SNF complex-induced activity (*lane 2* set as 100%). *B*, the pREP4-p53RE-luc was transfected with plasmid for mock or p53 in NIH3T3 cells. The effect of BAF60a160 was tested by co-transfecting increasing amounts of BAF60a160 expression vector (2, 5, and 10 μg for *lanes 3*, *4*, and *5*, respectively) with a fixed amount of p53 expression vector (1 μg). *C*, samples from *B* were Western blotted (*WB*) with antibodies for FLAG (*top*) and BAF60a (*bottom*) after luciferase assay in the same order as in *B*, *lanes 1–5*. *D*, the pREP4-p53RE-luc reporter was transfected with empty vector or expression vector for p53 in SaOS-2 cells. BAF60a160 expression vector (10 μg) was co-transfected with p53 expression vector (2 μg) to evaluate the effect of BAF60a160. Relative luciferase activities due to p53 are presented as a percentage of the SWI/SNF complex-induced activity (*lane 2* set as 100%). *Columns* in *A*, *B*, and *D* represent the mean ± S.D. ($n = 3$).

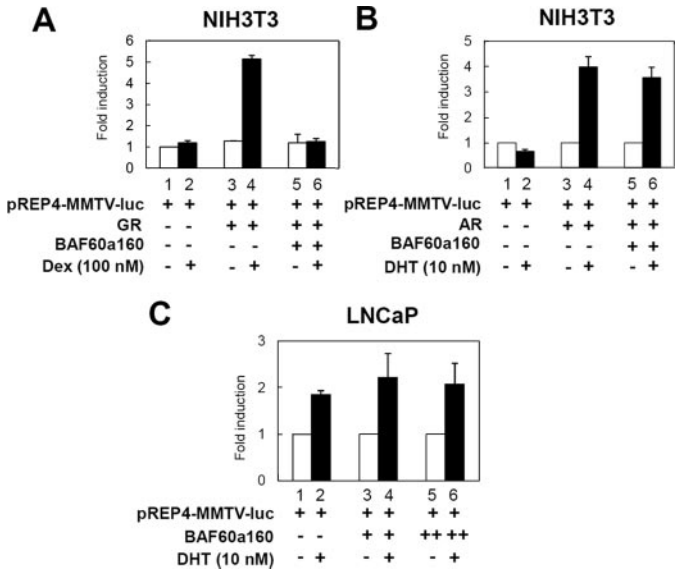

FIGURE 7. **BAF60a160 does not disrupt the functionality of the SWI/SNF complex.** *A*, NIH3T3 cells were co-transfected with pREP4-MMTV-luc (3 μg), GR (1 μg), or BAF60a160 (10 μg) vectors as indicated. Some cells were treated for the last 16 h prior to harvest with 100 nM dexamethasone (*DEX*; *lanes 2*, *4*, and *6*). Relative reporter activities are shown as the means of three independent experiments, each done in triplicate (*lane 1* set as 1-fold). *B*, NIH3T3 cells were co-transfected with pREP4-MMTV-luc (3 μg), AR (1 μg), or BAF60a160 (10 μg) as indicated. Some cells were treated for the last 16 h prior to harvest with 10 nM dihydrotestosterone (*DHT*; *lanes 2*, *4*, and *6*). Luciferase was assayed, calculated, and presented as the relative activity of *lane 1* to 1-fold. Shown are the means of three independent experiments, each done in triplicate. *C*, LNCaP cells were transfected with pREP4-MMTV-luc (3 μg). Some cells were co-transfected with BAF60a160 expression vector (+, 2.5 μg for *lanes 3* and *4*; ++, 5 μg for *lanes 5* and *6*) or treated for the last 16 h prior to harvest with 10 nM DHT (*lanes 2*, *4*, and *6*), as indicated. *Columns* represent relative reporter activity (*lane 1* set as 1-fold; $n = 3$).

dominant negative mutant that suppresses the SWI/SNF complex-mediated transcriptional activity of p53.

BAF60a160 Does Not Disrupt the Functionality of the SWI/SNF Complex—Although the deletion studies support the notion that the dominant negative effect of BAF60a160 is probably due to disruption of the linker function of BAF60a between p53 and the SWI/SNF complex, disruption of the intact SWI/SNF complex by BAF60a160 still remains a possibility. Therefore, we investigated whether the functionality of the SWI/SNF complex is maintained in the presence of BAF60a160. The SWI/SNF complex-mediated transcriptional activity of well characterized GR and AR was examined in the presence or absence of BAF60a160. GR and the SWI/SNF complex are linked by BAF60a, whereas AR and the SWI/SNF complex are mediated by BAF57 (10, 12). If BAF60a160 disrupts the functionality of the SWI/SNF complex, the SWI/SNF complex-mediated transcriptional activity of both AR and GR will be disrupted. On the other hand, if BAF60a160 specifically inhibits the linker activity of BAF60a without disrupting the SWI/SNF complex, AR-mediated transactivity will be maintained, whereas GR- and p53-mediated activities are repressed. To test this hypothesis, we first cloned the pREP4-MMTV-luc reporter in which the LTR sequence of MMTV is inserted as a promoter. The LTR sequence of MMTV has response elements for both GR and AR. The chromatin-structured pREP4-MMTV-luc reporter was activated by the SWI/SNF complex-mediated transcriptional activity of GR and AR when dexamethasone (*Dex*) and dihydrotestosterone (*DHT*) were treated as ligands, respectively (Fig. 7, *A* (*lane 4 versus lane 3*) and *B* (*lane 4 versus lane 3*)). However, the transcriptional activity of GR on the pREP4-MMTV-luc was significantly inhibited by co-expression of BAF60a160, whereas that of AR was not (Fig. 7, *A* (*lane 6 versus lane 4*) and *B* (*lane 6 versus lane 4*)). In AR-positive and the SWI/SNF complex-positive prostatic adenocarcinoma LNCaP cell line, endogenous AR-mediated transcription on the pREP4-MMTV-luc reporter was enhanced by the treatment of DHT (Fig. 7*C*, *lane 2 versus lane 1*). However, the transcriptional activity of AR was not affected despite the increasing amount of BAF60a160 expression vector transfected (Fig. 7*C*, *lanes 4* and *6 versus lane 2*). In conclusion, BAF60a160 specifically inhibited the BAF60a-mediated recruitment of the SWI/SNF complex without disrupting its functionality. These results indicate that BAF60a160 may interfere with the docking of transcription factors to BAF60a of the SWI/SNF complex.

p53-induced Apoptosis and Cell Cycle Arrest Are Also Alleviated by BAF60a160—We next examined if the interaction between p53 and the SWI/SNF complex is also crucial for p53 to exert its tumor-suppressing activity. Introduction of p53 is known to induce apoptosis in p53-deficient SaOS-2 cell line (37). Thus, we analyzed the effect of BAF60a160 on p53-dependent apoptosis in SaOS-2 cell line, in which the transcriptional activity of p53 had also been significantly down-regulated by BAF60a160 (Fig. 6*D*, *lane 3 versus lane 2*). The percentages

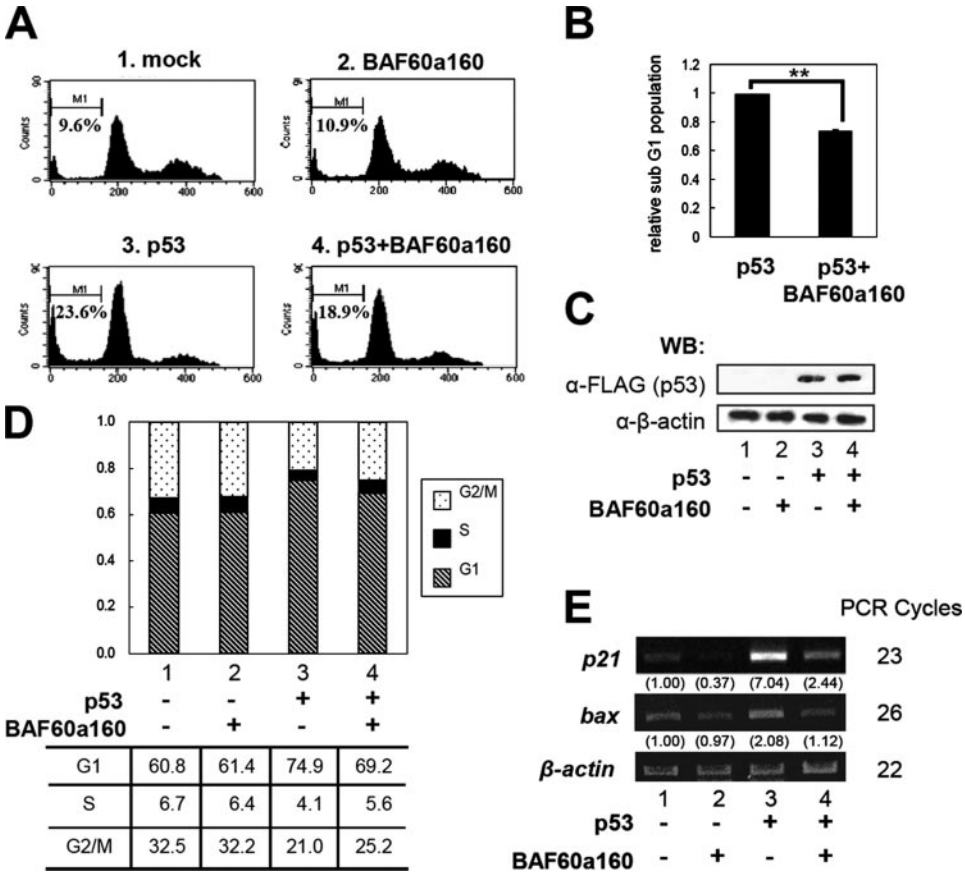

FIGURE 8. **BAF60a160 alleviates the p53-mediated apoptosis and cell cycle arrest in SaOS-2 cells.** SaOS-2 cells were transiently transfected with 12 μg of empty vector (*panel 1* and *lane 1* of *A* and *C*, respectively), 10 μg of BAF60a160 (*panel 2* and *lane 2*), 2 μg of p53 (*panel 3* and *lane 3*), or 10 μg of BAF60a160 and 2 μg of p53 expression vectors (*panel 4* and *lane 4*) for 60 h. *A*, cells were harvested, stained with PI, and subjected to flow cytometry. Sub-G_1 population was gated (M1) as apoptotic bodies, and their percentages are shown as *numbers below* the M1 gate. Results shown are representative of three independent experiments with similar results. *B*, the relative sub-G_1 population was calculated and plotted ($n = 3$). The *left column* corresponds to the value of *panel 3* of *A* divided by that of *panel 1*, and the *right column* corresponds to the value of *panel 4* divided by that of *panel 2*. Note that the value of the *left column* is set as *1*. **, significance was $p < 0.01$ for *t* test. *C*, whole cell extracts were subjected to immunoblotting (*WB*) with the indicated antibodies. β-Actin was used as a loading control (*bottom*). This is a representative of three similar results. *D*, only the live cells were gated to determine the percentage of cells in the G_1, S, and G_2/M phases of the cell cycle. Note that the sub-G_1 population, which corresponded to M1 gates of *A*, was excluded in gatings and subsequent calculations. Results shown are representative of similar results. *E*, total RNAs of *A* were subjected to RT-PCR with primers specific for the genes shown on the *left* of each *panel*. β-Actin was used as a loading control. Relative mRNA amounts are represented in *parenthesis*, and PCR cycles are indicated at the *right*.

of sub-G_1 population, which represents the apoptotic bodies, were similar at ~10% in both mock- and BAF60a160-transfected cells (Fig. 8*A*, *panels 1* and *2*). Although the expression of exogenous p53 resulted in enhanced sub-G_1 population (Fig. 8*A*, *panel 3 versus panel 1*), the addition of BAF60a160 partially reversed the enhancement (Fig. 8*A*, *panel 4 versus panel*). Statistical analysis of three independent experiments yielded a 27% reduction in sub-G_1 population by BAF60a160 (Fig. 8*B*). p53 protein level was not affected by the co-expression of BAF60a160 (Fig. 8*C*, *lane 3 versus lane 4*). We next examined the effect of BAF60a160 on cell cycle progression, since SaOS-2 cells transfected with wild-type p53 are unable to progress into S phase and arrest in G_1 phase (38). Cell cycle distribution of transfected SaOS-2 cells as in Fig. 8*A* was assessed by PI staining and flow cytometry. As shown in Fig. 8*D*, mock- and BAF60a160-transfected cells gave similar cell cycle distribution patterns (*lanes 1* and *2*). However, p53-transfected cells displayed a significant increase in G_1 phase and a decrease in S phase (Fig. 8*D*, *lane 3 versus lane 1*), which was partially reversed by co-expression of BAF60a160 (Fig. 7*D*, *lane 4 versus lane 3*). Because such results are probably due to changes in p53-mediated transcription of cell cycle and apoptotic regulators, we next examined the effect of BAF60a160 on the transcription of few known regulators. Expression of p53 alone in SaOS-2 cells resulted in enhanced expression of *p21* and *bax* at the transcript levels (Fig. 8*E*, *lane 3 versus lane 1*), but co-expression of p53 and BAF60a160 yielded significantly reduced expression (Fig. 8*E*, *lane 4 versus lane 3*). p53-mediated target gene expression was also repressed by BAF60a160.

To investigate the effect of BAF60a160 on p53-mediated apoptosis in a more physiological setting, we introduced BAF60a160 expression vector by the retroviral transduction and induced endogenous apoptosis by treatment of doxorubicin. Since the retroviral construct contained internal ribosome entry site sequence followed by green fluorescence protein (GFP), GFP-positive cells are those transduced with the retroviral vector. When we compared apoptotic induction between the GFP-positive population of vector- and BAF60a160-transduced cells at the 24 and 48 h time points, induction of apoptosis was inhibited in BAF60a160-transduced cells at both time points (Fig. 9*B*). However, the degree of apoptotic induction was similar in GFP-negative populations (Fig. 9*C*).

To further evaluate the physiological relevance of BAF60a in mediating the endogenously induced apoptosis, we established NIH3T3 cells that express low and high levels of BAF60a160 and analyzed the dose-dependent effect of BAF60a160 on doxorubicin-mediated apoptosis (Fig. 9*D*). When we treated doxorubicin and measured the percentage of annexin V-positive population at the 24 and 48 h time points, doxorubicin-induced apoptosis was repressed in correspondence to the expression level of BAF60a160 (Fig. 9*E*).

Taken together, BAF60a160 acts dominant negatively on p53-mediated apoptosis and cell cycle arrest by attenuating the SWI/SNF complex-aided transcriptional activity of p53 on target regulatory genes.

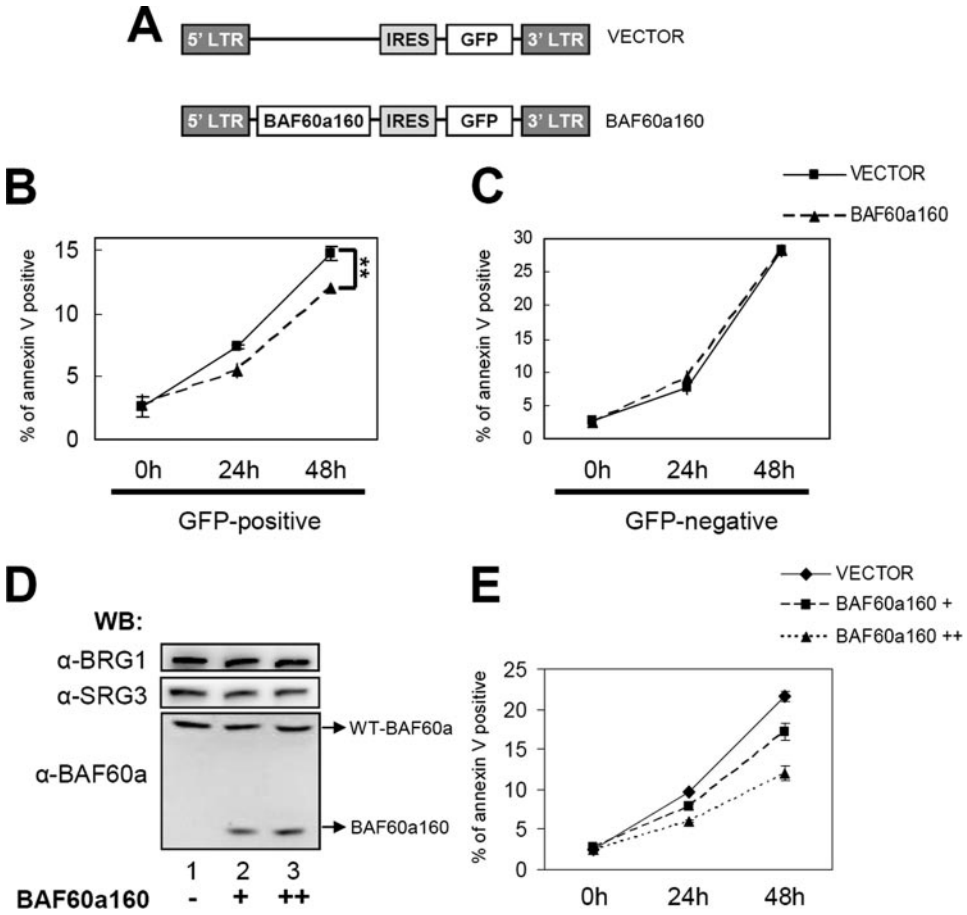

FIGURE 9. **Doxorubicin-induced apoptosis is also repressed in BAF60a160-transduced NIH3T3 cells.** *A*, schematic illustration of retroviral vectors. To construct BAF60a160-expressing retroviral vector, cDNA for *baf60a160* was inserted into MigRI vector. *IRES*, internal ribosome entry site; *GFP*, green fluorescence protein. *B* and *C*, NIH3T3 cells were retrovirally transduced with mock- or BAF60a160-vector. At 36 h post-transduction, 1 μg/ml doxorubicin was treated for 0 h (*0h*), 24 h (*24h*), and 48 h (*48h*). Cells were harvested and stained with annexin V-PE antibody to analyze by flow cytometry. GFP-positive (*B*) and -negative (*C*) populations were gated separately. The percentage of annexin V-positive cells in each population is plotted and shown with *error bars* (S.D.; $n = 3$). **, significance at the 48 h time point, $p < 0.02$ for *t* test (*B*). *D* and *E*, BAF60a160-expressing NIH3T3 cells were established after transfection of mock and 2 and 5 μg of pcDNA3-BAF60a160 expression vectors. Those three cell populations were selected with G418 (1 mg/ml) for 3 weeks. Pooled cells were harvested and subjected to immunoblotting (*WB*) with the indicated antibodies (*D*). Mock (*VECTOR*), BAF60a160+, and BAF60a160++ cells were treated with 1 μg/ml doxorubicin for 0 h (*0h*), 24 h (*24h*), and 48 h (*48h*). At each time point, cells were harvested and stained with annexin V-PE antibody to analyze by flow cytometry. The percentage of annexin V-positive population is represented as a *graph* with *error bars* (S.D.; $n = 3$) (*E*).

DISCUSSION

Our results demonstrate that p53 requires the interaction with the SWI/SNF complex to induce transcription from the nucleosomal promoter. p53-responsive elements packaged in the nucleosomal structure were hardly activated by p53 until the functional SWI/SNF complex was reconstituted by the restoration of BRG1 in the SW-13 cell line. Notably, this enhancement of transcriptional activity of p53 was dependent on its protein-protein interaction with the SWI/SNF complex. The disruption of the interaction by the down-regulation or by the dominant negative form of the linker significantly reduced the SWI/SNF complex-mediated transcriptional activity of p53 and the p53-dependent effects as a result.

Among p53 target genes, we strongly suggest *p21* as a p53 target gene that requires the chromatin remodeling activity of the SWI/SNF complex for p53-mediated transcription. In SW-13 cell line, we investigated few p53 target genes but found no other genes that were dramatically changed like *p21*. It was previously reported that the reconstitution of the SWI/SNF complex in the SW-13 cell line induces *p21* expression independently of p53 (33, 40). Although transfection of either p53 or BRG1 yielded minor induction of *p21* expression, co-transfection of BRG1 and p53 gave substantial induction of *p21* expression (Fig. 1*F*). Thus, although expression of *p21* could also be induced by the SWI/SNF complex independently of p53 in some situations, cooperation between the SWI/SNF complex and p53 seems to be the major mechanism of inducing *p21* in response to stresses.

BAF60a, among the core components of the SWI/SNF complex, is shown here as the mediator of interaction between the SWI/SNF complex and p53. We were not able to find direct interaction between p53 and the other core subunits of the SWI/SNF complex, including BRG1 and SNF5, although they have previously been reported to interact with p53 by immunoprecipitation and the GST pull-down assay (27). Our results suggest BRG1 and SNF5 to be co-purified with p53 through indirect interaction mediated by BAF60a in the cell extracts or the reticulocyte lysates (39). Although the involvement of the unexamined components of the SWI/SNF complex cannot be completely excluded, the effect of si-*baf60a* and the dominant negative effect of BAF60a160 strongly support the bridging role of BAF60a between p53 and the SWI/SNF complex. Unlike the effect of si-*baf60a* and BAF60a160 on the transcriptional activity of p53, overexpression of wild-type BAF60a did not enhance the transcriptional activity in either the transient reporter or the nucleosomal reporter in various cell lines (data not shown). This result suggests that BAF60a does not have either a cofactor function on p53 by itself or an additive role for the chromatin remodeling activity of the SWI/SNF complex. Taken together, BAF60a seems to be the mediator between p53 and the SWI/SNF complex.

The N-terminal aa 108–150 region of BAF60a distinct from the SWIB/MDM2 domain was mapped to be involved in the interaction with p53. BAF60aΔ108–150, which lacks the p53-interacting region, did not interact with p53 either in the yeast two-hybrid or immunoprecipitation assays. These results coin-

cide with earlier studies that report the N terminus of BAF60a as the interacting region with various transcription factors (12–14, 16, 17). Although a substantial amount of studies report BAF60a as a mediator, no study has mapped the interacting region at the amino acid level. To unveil the mechanism of versatile interaction of BAF60a, we tried to narrow down the p53-interacting region to the amino acid level. Although both the aa 108–113 and aa 142–150 regions of BAF60a were shown to contain the interacting residue(s) for p53, either deletion of the interacting region or the partial deletion of the interacting region did not abrogate the interaction with p53. Thus, multiple residues in aa 108–150 of BAF60a seem to be engaged in the interaction with p53.

There is no known domain in the aa 108–150 region of BAF60a; however, the region is rich with charged residues (40% of aa among aa 108–150 are charged aa) and is predicted to form a structure that consists of helixes and strands (analyzed with PSIPRED, Protein Structure Prediction Server). Thus, we suggest that other sets of multiple charged residues among aa 108–150 may also be engaged in the interaction with other transcription factors. Therefore, we can further suggest that BAF60a160 may disrupt the interaction between the SWI/SNF complex and other transcription factors, as well as GR and p53, which are known to be mediated by BAF60a (12). Notably, BAF60a160 inhibited the SWI/SNF complex-mediated activation linked by BAF60a without disabling the SWI/SNF complex. The transcriptional activity of p53 and GR was repressed by BAF60a160, whereas that of AR was not. Thus, the N-terminal fragment of BAF60a seems to be the dominant negative inhibitor that specifically inhibits the interactions toward BAF60a.

Many studies have reported the relationship between cancer and mutations in components of the SWI/SNF complex (5). Lack of certain components within the SWI/SNF complex increases the cancer susceptibility in mice, and mutations in components are being identified in various cancer cell lines (3, 41–43). This tumor-suppressing activity of the SWI/SNF complex has been elucidated in relation to RB, BRCA1, and c-MYC, but these have not been enough to fully explain the prognosis of mutations of the SWI/SNF components (5, 9, 30, 31). Here, we show that p53 was not able to fully exert its anti-tumor function, induction of apoptosis and arrest of cell cycle, when the interaction with the SWI/SNF complex was disrupted by the dominant negative form of BAF60a or suppressed by *baf60a*-specific siRNA. Although the relationship between the occurrence of cancer and mutations in BAF60a is not reported yet, our study suggests that mutation in BAF60a may be implicated in the tumorization, particularly in cancers with wild-type p53. In conclusion, our study not only demonstrates BAF60a-mediated interaction between the SWI/SNF complex and p53 but also suggests a tumor-suppressing mechanism of the SWI/SNF complex in relation to p53.

REFERENCES

1. Kwon, H., Imbalzano, A. N., Khavari, P. A., Kingston, R. E., and Green, M. R. (1994) *Nature* **370,** 477–481
2. Sudarsanam, P., and Winston, F. (2000) *Trends Genet.* **16,** 345–351
3. Bultman, S., Gebuhr, T., Yee, D., La Mantia, C., Nicholson, J., Gilliam, A., Randazzo, F., Metzger, D., Chambon, P., Crabtree, G., and Magnuson, T. (2000) *Mol. Cell* **6,** 1287–1295
4. Kim, J. K., Huh, S. O., Choi, H., Lee, K. S., Shin, D., Lee, C., Nam, J. S., Kim, H., Chung, H., Lee, H. W., Park, S. D., and Seong, R. H. (2001) *Mol. Cell. Biol.* **22,** 7787–7795
5. Roberts, C. W., and Orkin, S. H. (2004) *Nat. Rev. Cancer* **4,** 133–142
6. Wang, W., Xue, Y., Zhou, S., Kuo, A., Cairns, B. R., and Crabtree, G. R. (1996) *Genes Dev.* **17,** 2117–2130
7. Wang, W., Cote, J., Xue, Y., Zhou, S., Khavari, P. A., Biggar, S. R., Muchardt, C., Kalpana, G. V., Goff, S. P., Yaniv, M., Workman, J. L., and Crabtree, G. R. (1996) *EMBO J.* **19,** 5370–5382
8. Sohn, D. H., Lee, K. Y., Lee, C., Oh, J., Chung, H., Jeon, S. H., and Seong, R. H. (2007) *J. Biol. Chem.* **282,** 10614–10624
9. Cheng, S. W., Davies, K. P., Yung, E., Beltran, R. J., Yu, J., and Kalpana, G. V. (1999) *Nat. Genet.* **22,** 102–1055
10. Link, K. A., Burd, C. J., Williams, E., Marshall, T., Rosson, G., Henry, E., Weissman, B., and Knudsen, K. E. (2005) *Mol. Cell. Biol.* **25,** 2200–2215
11. Belandia, B., Orford, R. L., Hurst, H. C., and Parker, M. G. (2002) *EMBO J.* **21,** 4094–4103
12. Hsiao, P. W., Fryer, C. J., Trotter, K. W., Wang, W., and Archer, T. K. (2003) *Mol. Cell. Biol.* **23,** 6210–6220
13. Debril, M., Gelman, L., Fayard, E., Annicotte, J., Rocchi, S., and Auwerx, J. (2004) *J. Biol. Chem.* **279,** 16677–16686
14. Ito, T., Yamauchi, M., Nishina, M., Yamamichi, N., Mizutani, T., Ui, M., Murakami, M., and Iba, H. (2001) *J. Biol. Chem.* **276,** 2852–2857
15. Koszewski, N. J., Henry, K. W., Lubert, E. J., Gravatte, H., and Noonan, D. J. (2003) *J. Steroid Biochem. Mol. Biol.* **87,** 223–231
16. Assmann, E. M., Alborghetti, M. R., Camargo, E. R., and Kobarg, J. (2006) *J. Biol. Chem.* **281,** 9869–9881
17. Chien, C. Y., Liu, W. K., Chou, C. K., and Su, J. Y. (2003) *FEBS Lett.* **543,** 55–60
18. Felsenfeld, G. (1992) *Nature* **335,** 219–224
19. Trotter, K. W., and Archer, T. K. (2007) *Mol. Cell. Endocinol.* **265,** 162–167
20. Trotter, K. W., and Archer, T. K. (2004) *Mol. Cell. Biol.* **24,** 3347–3358
21. Hong, C. Y., Suh, J. H., Kim, K., Gong, E. Y., Jeon, S. H., Ko, M., Seong, R. H., Kwon, H. B., and Lee, K. (2005) *Mol. Cell. Biol.* **25,** 4841–4852
22. Levine, A. J. (1997) *Cell* **88,** 323–331
23. Espinosa, J. M., and Emerson, B. M. (2001) *Mol. Cell* **8,** 57–69
24. Barlev, N. A., Liu, L., Chehab, N. H., Mansfield, K., Harris, K. G., Halazonetis, T. D., and Berger, S. L. (2001) *Mol. Cell* **8,** 1243–1254
25. Murphy, M., Ahn, J., Walker, K. K., Hoffman, W. H., Evans, R. M., Levine, A. J., and George, D. L. (1999) *Genes Dev.* **13,** 2490–2501
26. An, W., Kim, J., and Roeder, R. G. (2004) *Cell* **117,** 735–748
27. Lee, D., Kim, J. W., Seo, T., Hwang, S. G., Choi, E. J., and Choe, J. (2002) *J. Biol. Chem.* **277,** 22330–22337
28. Kim, D., Xu, M., Nie, L., Peng, X. C., Jimi, E., Voll, R. E., Nguyen, T., Ghosh, S., and Sun, X. H. (2002) *Immunity* **16,** 9–21
29. Han, S., Choi, H., Ko, M. G., Choi, Y. I., Sohn, D. H., Kim, J. K., Shin, D., Chung, H., Lee, H. W., Kim, J. B., Park, S. D., and Seong, R. H. (2001) *J. Immunol.* **167,** 805–810
30. Dunaief, J. L., Strober, B. E., Guha, S., Khavari, P. A., Alin, K., Luban, J., Begemann, M., Crabtree, G. R., and Goff, S. P. (1994) *Cell* **79,** 119–130
31. Bochar, D. A., Wang, L., Beniya, H., Kinev, A., Xue, Y., Lane, W. S., Wang, W., Kashanchi, F., and Shiekhattar, R. (2000) *Cell* **102,** 257–265
32. Liu, R., Liu, H., Chen, X., Kirby, M., Brown, P. O., and Zhao, K. (2001) *Cell* **106,** 309–318
33. Kang, H., Cui, K., and Zhao, K. (2004) *Mol. Cell. Biol.* **24,** 1188–1199
34. van der Vlag, J., den Blaauwen, J. L., Sewalt, R. G., van Driel, R., and Otte, A. P. (2000) *J. Biol. Chem.* **275,** 697–704
35. Zhao, K., Wang, W., Rando, O. J., Xue, Y., Swiderek, K., Kuo, A., and Crabtree, G. R. (1998) *Cell* **95,** 625–636
36. Bennett-Lovsey, R., Hart, S. E., Shirai, H., and Mizuguchi, K. (2002) *Bioinformatics* **18,** 626–630
37. Chen, P. L., Chen, Y. M., Bookstein, R., and Lee, W. H. (1990) *Science* **250,** 1576–1580
38. Driller, L., Kassel, J., Nelson, C. E., Gryka, M. A., Litwak, G., Gebhardt, M., Bressac, B., Ozturk, M., Baker, S. J., Vogelstein, B., and Friend, S. H. (1990) *Mol. Cell. Biol.* **10,** 5772–5781

39. Huibregtse, J. M., Scheffner, M., and Howley, P. M. (1991) *EMBO J.* **10,** 4129–4135
40. Hendricks, K. B., Shanahan, F., and Lees, E. (2004) *Mol. Cell. Biol.* **24,** 362–376
41. Versteege, I., Sevenet, N., Lange, J., Rousseau-Merck, M. F., Ambros, P., Handgretinger, R., Aurias, A., and Delattre, O. (1998) *Nature* **394,** 203–206
42. Biegel, J. A., Zhou, J. Y., Rorke, L. B., Stenstrom, C., Wainwright, L. M., and Fogelgren, B. (1999) *Cancer Res.* **59,** 74–79
43. Kiskinis, E., Garcia-Pedrero, J. M., Villaronga, M. A., Parker, M. G., and Belandia, B. (2006) *Breast Cancer Res. Treat.* **98,** 191–198
44. Ko, M., Ahn, J., Lee, C., Chung, H., Jeon, S. H., Chung, H. Y., and Seong, R. H. (2004) *J. Biol. Chem.* **279,** 21916–21923
45. Miyashita, T., and Reed, J. C. (1995) *Cell* **80,** 293–299